

# 7

## FINITE ELEMENT METHOD IN THE THERMAL BUCKLING ANALYSIS OF ANISOTROPIC PLATES

citation and similar papers at [core.ac.uk](http://core.ac.uk)

provided by Universiti Teknologi

### 7.0 INTRODUCTION

Fibre reinforced composite (FRC) is a popular choice in structural designs that require weight saving. To meet this requirement, FRC components are usually thin and curvy. This will create problems especially when the FRC components are subjected to compressive mechanical and thermal loads. One such problem is the thermal buckling and post-buckling that typically occurs in these composite plates. Thermal buckling of plate structures is a sudden huge lateral deflection that occurs when the temperatures of the plates are increased above the critical temperature,  $T_{cr}$ . This phenomenon may result in the reduction of the performance of the respected components or even causing total failure of the whole structure. As such, thermal loading is an important design consideration especially for structures like high speed aircrafts, rockets and launch vehicles. In this case, thermal loading is caused by aerodynamic heating which is due to supersonic or hypersonic flight. This heating will provide the structure's external skin with thermal compressive load since the inner part of the skin remains cooler and thus restrains the free expansion of the skin. As a result the outer skin will be subjected to thermal buckling because of the typical low thickness in the FRC components [1].

Recently, studies on thermal buckling and post-buckling were

conducted by Thankam et. al.[2]. While employing the finite element method, they used the shear-flexible element based on coupled-displacement field. Several patterns of thermal buckling behaviours validated using the result from past researches proved the applicability of the used model. Thermal buckling of laminated composite plates was studied using the finite element method by M.R. Prabhu and R. Dhanaraj [3]. The parametric studies of the thermal buckling analysis on the symmetric angle-ply and cross-ply and the quasi-isotropic laminates were conducted. The influence of the stress distribution on the variation of critical temperature with fibre orientation was studied for different boundary conditions. It was found among others that the variation of  $T_{cr}$  is not symmetric with respect to  $\theta = 45^0$  for a symmetric angle-ply laminates. Similar studies were also conducted by C.A. Shankara and N.G.R. Iyengar [4]. They however used both the higher order shear deformation theory (HSDT) and the FSDT of composites to describe the kinematics of the composites. As such, similar results to [3] were obtained. J.S. Chang [5] used the higher order theory of laminated composites, taking into account the transverse normal strain effect to model the kinematics of composites in studying its thermal buckling behaviours. The effects of important parameters such as ply angle, ratio of thickness to edge length and number of layers were studied. Chen et. al.[6] enhanced the studies on thermal buckling of composite plates by considering the non-uniform temperature distribution. It was found that the effects of the lamination angles, the anisotropy, aspect ratios and boundary conditions upon the critical temperatures were significant.

These papers report the initial stage of the intended study on the non-linear post-buckling analysis of smart composite plates. It covers the thermal buckling behaviours of laminated composite plates. The non-linear finite element model of composite plates was first developed using the kinematical theory of the FSDT. Then the obtained finite element governing equation was reduced to the linear thermal buckling analysis which is the linear eigen-value problem. The source codes were then developed where at the end, the inverse power method was used to solve the critical temperatures of the plates. Parametric studies were conducted on these thermal buckling behaviours of composite plates using several parameters such as the number of layers, aspect ratios, side to thickness ratios and boundary conditions. The determined patterns of behaviours then are useful to the designs of composite plates that involve thermal effect.

## 7.1 FINITE ELEMENT MODEL DEVELOPMENT

The in-plane constitutive relationship for a composite plate in the material coordinate system (system-123) is

$$\begin{Bmatrix} \sigma_1 \\ \sigma_2 \\ \sigma_{12} \end{Bmatrix} = \begin{bmatrix} Q_{11} & Q_{12} & 0 \\ Q_{12} & Q_{22} & 0 \\ 0 & 0 & Q_{33} \end{bmatrix} \begin{Bmatrix} \varepsilon_1 \\ \varepsilon_2 \\ \gamma_{12} \end{Bmatrix} - \begin{Bmatrix} \alpha_1 \\ \alpha_2 \\ 0 \end{Bmatrix} \Delta T \quad (1a)$$

or in a short form,

$$\{\sigma_1\} = [Q]\{\varepsilon_1\} - \{\alpha_1\} \Delta T \quad (1b)$$

where  $[Q]$  is the reduced stiffness matrix of the composite [7],  $\{\sigma_1\}$ ,  $\{\varepsilon_1\}$  and  $\{\alpha_1\}$  are the vectors of stress, strain and thermal coefficient of expansion in the material coordinate system respectively and  $\Delta T$  is the change in temperature. For the constitutive relationship in the transverse direction, refer to [7]. Using the transformation matrix [6] we have,

$$\{\sigma_x\} = [\bar{Q}]\{\varepsilon_x\} + \{\alpha_x\} \Delta T \quad (2)$$

where  $[\bar{Q}]$  is the transformed reduced stiffness matrix of the composites, and  $\{\sigma_x\}$ ,  $\{\varepsilon_x\}$  and  $\{\alpha_x\}$  are the vectors of stress, strain and thermal coefficient of expansion in the Cartesian coordinate system (xyz-system). Using the Mindlin's FSDT [7], displacements at any points in laminated composite plates can be expressed as,

$$u(x,y,z,t) = u_o(x,y,t) + z \theta_x(x,y,t)$$

$$\begin{aligned} v(x,y,z,t) &= v_o(x,y,t) + z \theta_y(x,y,t) \\ w(x,y,z,t) &= w_o(x,y,t) \end{aligned} \quad (3)$$

where  $u_o$ ,  $v_o$  and  $w_o$  are the mid-plane displacements in the x, y and z directions respectively while  $\theta_x$  and  $\theta_y$  are the normal rotations in the xz-planes and yz-planes respectively and t is the time variable. By including the von Karman's strain, the strain can be expressed as

$$\{\varepsilon\} = \{\varepsilon_{xx}, \varepsilon_{yy}, \varepsilon_{zz}\}^T \quad (4a)$$

$$= \begin{Bmatrix} \frac{\partial u}{\partial x} \\ \frac{\partial v}{\partial y} \\ \frac{\partial u}{\partial y} + \frac{\partial v}{\partial x} \end{Bmatrix} + \frac{1}{2} \begin{Bmatrix} \left(\frac{\partial w}{\partial x}\right)^2 \\ \left(\frac{\partial w}{\partial y}\right)^2 \\ 2\left(\frac{\partial w}{\partial x}\right)\left(\frac{\partial w}{\partial y}\right) \end{Bmatrix} + z \begin{Bmatrix} \frac{\partial \theta_x}{\partial x} \\ \frac{\partial \theta_y}{\partial y} \\ \left(\frac{\partial \theta_x}{\partial y} + \frac{\partial \theta_y}{\partial x}\right) \end{Bmatrix} \quad (4b)$$

or

$$\{\varepsilon\} = \{\varepsilon_p\} + z\{\kappa\} = \{\varepsilon_m\} + \{\varepsilon_{nl}\} + z\{\kappa\} \quad (4c)$$

where  $\{\varepsilon_m\}$ ,  $\{\varepsilon_{nl}\}$  and  $\{\kappa\}$  are the in-plane linear strain vector, the in-plane non-linear strain vector and the curvature strain vector, respectively. The transverse shear strain vector is as the following.

$$\{\gamma\} = \begin{Bmatrix} \gamma_{xz} \\ \gamma_{yz} \end{Bmatrix} = \begin{Bmatrix} \frac{\partial w}{\partial x} + \theta_y \\ \frac{\partial w}{\partial y} + \theta_x \end{Bmatrix} \quad (5)$$

Defining stress resultants in the usual ways [7], we have a constitutive relationship regarding the in-plane stress

$$\begin{Bmatrix} \{N\} \\ \{M\} \end{Bmatrix} = \begin{bmatrix} [A] & [B] \\ [B] & [D] \end{bmatrix} \left( \begin{Bmatrix} \{\varepsilon_m\} \\ \{\kappa\} \end{Bmatrix} + \begin{Bmatrix} \{\varepsilon_{nl}\} \\ 0 \end{Bmatrix} \right) + \begin{Bmatrix} \{N_T\} \\ \{M_T\} \end{Bmatrix} \quad (6)$$

and for the out of plane stress,

$$\{Q\} = \begin{Bmatrix} Q_{xz} \\ Q_{yz} \end{Bmatrix} = \begin{bmatrix} A_{44} & A_{45} \\ A_{45} & A_{55} \end{bmatrix} \{\gamma\} = [A'] \{\gamma\} \quad (7)$$

where  $[A]$ ,  $[B]$ ,  $[D]$  and  $[A']$  are the material matrices of the laminate while  $\{N\}$  and  $\{M\}$  are the force and moment resultant vectors, respectively.  $\{N_T\}$  and  $\{M_T\}$  are the resultant force and moment vectors due to the change in temperatures respectively such as

$$(\{N_T\}, \{M_T\}) = \sum_{n=1}^k \int_{-t/2}^{t/2} [\bar{Q}] \{\alpha_x\} \Delta T(1, z) dz \quad (8)$$

where  $\{\alpha_x\}$  is the thermal coefficient of expansion vector in xyz-coordinate system and  $k$  is the total number of layer of the composite. Eight noded isoparametric quadrilateral elements are used here. Each node carries 5 degrees of freedom.

$$\{a\} = [N] \{q\} \quad (9)$$

$$\{q\}^T = \{u_1, v_1, w_1, \theta_{x1}, \theta_{y1}, u_2, \dots, w_8, \theta_{x8}, \theta_{y8}\} \quad (10)$$

where  $\{a\}$  and  $\{q\}$  are the generalised and nodal displacement column matrices and  $[N]$  is the shape function matrix. The principle of virtual works can be stated as

$$\delta W = \delta W_{int} - \delta W_{ext} = 0 \quad (11)$$

$$\delta W_{int} = \{\delta q\}^T \int_A \left\{ \delta \varepsilon_m \right\}^T \{N\} + \left\{ \delta \varepsilon_{nl} \right\}^T \{N\} + \left\{ \varepsilon_b \right\}^T \{M\} + \left\{ \varepsilon_s \right\}^T \{Q\} dA \quad (12)$$

Following the standard FEM procedures [6], we have

$$\delta w_{\text{int}} = \{\delta q\}^T \left( [K_L] + [K_s] - [K_T] + [K_G] + \frac{1}{2}[N_1] + \frac{1}{3}[N_2] \right) \{q\} - \{\delta q\}^T \{P_T\} \quad (13)$$

where  $[K_L]$ ,  $[K_s]$ ,  $[K_T]$  and  $[K_G]$  are the linear, shear, thermal and geometric stiffness matrices.  $[N_1]$  and  $[N_2]$  are the first-order and second-order non-linear stiffness matrices and  $\{P_T\}$  is the thermal load vector. Since there are no external loads, the FEM governing equation for the non-linear buckling problem of SMA composite plates can be written as in the following.

$$\left( [K_L] + [K_s] - [K_T] + [K_G] + \frac{1}{2}[N_1] + \frac{1}{3}[N_2] \right) \{q\} = \{P_T\} \quad (14)$$

Equation (14) can be reduced to the equation for the linear thermal loading such as

$$([K_L] + [K_s])\{q\} = \{P_T\} \quad (15)$$

and to the equation for the linear thermal buckling problem of SMA composite plates as shown below.

$$([K_L] + [K_s] + [\lambda K_G])\{q\} = \{0\} \quad (16)$$

Equation (16) is an eigen-value problem. It can be solved by solving equation (15) for a very small change of temperature,  $\Delta T_{\text{ref}}$ . The resulting strains from this problem solution are then used to construct the geometric stiffness matrix so that equation (16) can be solved. The eigen-value of the equation (16) will give the critical temperature for the plates under consideration such as

$$\Delta T_{cr} = \lambda \Delta T_{ref} \quad (17)$$

Following this, source codes were developed to solve equation (15)-(17). Figure 7.1 shows the flow chart that is used in developing this source codes.

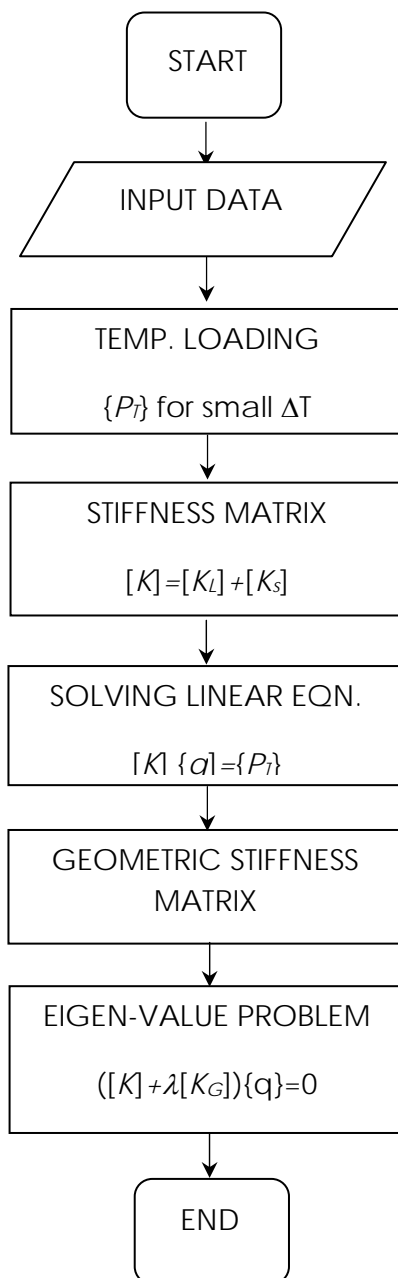


**Figure 7.1.** The flow chart for the development of the source codes for the thermal buckling of composites.

## 7.2 RESULTS AND DISSCUSSION

In this study except for the case of the effect of the number of layers, eight layer angle-ply composite plates are used. The symmetric angle-ply composites are of the form  $[\theta/-\theta/\theta/-\theta]_s$  while the anti-symmetric composites are of the form  $[\theta/-\theta]_4$ . Referring to Figure 7.2, that shows a composite plate to be modeled,  $a$  and  $b$  are side lengths of the plate and  $t$  is the plate thickness. Figure 7.2 also shows the xyz-coordinate as a typical Cartesian coordinate system while the 123-system is the material coordinate system.

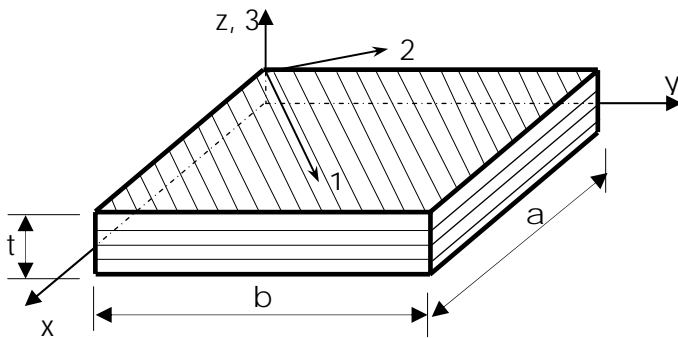


**Figure 7.2.** The laminated composite plates to be modeled.

Also in this study,  $E$  stands for the Young Modulus,  $\nu$  is the Poisson's ratio and  $\alpha$  is the thermal coefficient of expansion of the plate. The properties of isotropic plates [8] to be analysed are:

$$a/t=100, E=1.0, \nu=0.3, \alpha=1.0E-6$$

The properties of the orthotropic plates are:

$$a/b=1, a/t=100, E_1/E_2=40.0, G_{12}/E_2=0.6, G_{13}=G_{12},$$



$$G_{23}/E_2=0.5 \quad \nu_{12}=0.25, \quad \alpha_2/\alpha_1=10.0, \quad \alpha_1=1 \times 10^{-6}$$

There are three types of boundary conditions used in this study: Simply supported (SS), Hinged (HH) and Clamped (CC). Representing 1 as a zero displacement and 0 as an allowed displacement and following the order of degree of freedom in  $\{q\}$  in equation (10), the boundary conditions are

1. SS - at  $x=0$ , a: 01101, at  $y=0$ , b: 10110.
2. HH - at  $x=0$ , a: 11101, at  $y=0$ , b: 11110.
3. CC - at  $x=0$ , a: 11111, at  $y=0$ , b: 11111.

In most cases, the thermal critical loads are non-dimensionalised such as

$$NDT_{cr} = \alpha T_{cr} (a/t)^2 \quad (18)$$

Firstly, the validation of the developed model was made for the case of isotropic plates. The SS type boundary condition was used here. Table 1 shows the results of the  $NDT_{cr}$  for different  $a/b$  ratios of plates that agree excellently to the results of [7].

Secondly, convergence tests are conducted on composite plates to determine the appropriate mesh size for the thermal buckling analysis. At the same time the tests provide the validation to the finite element model developed for the case of orthotropic plates. The results such as shown in the Table 2 are compared to the past results [8] that are based on a different kinematical model of composite plates. The HH type boundary condition is used in the convergence tests for angle-ply composites while for cross-ply composites the CC type boundary condition is used. Table 2 shows that quick convergence occurs for the  $NDT_{cr}$  corresponding to the anti-symmetric composite plates while the  $NDT_{cr}$  correspond to the anti-symmetric cross-ply and symmetric angle-ply show a rather slow convergence. It was then decided in this study to use the 8x8 mesh of the plates instead.

**Table 1.** NDTcr for simply supported isotropic plates

a/b	NDT <sub>cr</sub>	
	Boley & Winer [7]	Present
0.25	<b>0.686</b>	0. 686
0.5	<b>0.808</b>	0.808
1.0	<b>1.283</b>	1.283
1.5	<b>2.073</b>	2.073
2.0	<b>3.179</b>	3.179
2.5	<b>4.599</b>	4.599
3.0	<b>6.332</b>	6.332

**Table 2.** Convergence test for the thermal buckling analysis of composite plates

Ply	NDT <sub>cr</sub>		
	(30/-30) <sub>s</sub>	(30/-30) <sub>2</sub>	(0/90) <sub>2</sub>
4x4	9.2002	10.2097	24.4680
5x5	8.7348	10.1779	24.4680
6x6	8.5804	10.1681	21.7432
7x7	8.5122	10.1640	21.6155
8x8	8.4307	10.1617	21.5720
10x10	8.4282	10.1598	21.5460

12x12	8.4192	10.1588	21.5390
<b>[8]</b>	<b>8.3957</b>	<b>10.1694</b>	<b>21.1663</b>

Next, studies on the effects of several parameters on the thermal buckling loads of angle-ply composite plates were conducted. Here the angles of orientation in the angle-ply composite plates were varied to see the change in the NDTcr that corresponds to each angle when the variation of several parameters occurs.

1.2.1 The effect of the number of layers

The symmetric angle-ply composite plates, for example with 3 layers are of the form  $[\theta/-\theta/\theta]$  while the form for the 7 layer composite is  $[\theta/-\theta/\theta/-\theta/\theta/-\theta/\theta]$ . The anti-symmetric angle-ply composite plates on the other hand are of the form  $[\theta/-\theta]_n$  where  $n = 1, 2$  and  $4$ . The HH boundary condition is used here. Figure 7.3 shows the effect of the number of layers for thin symmetric and anti-symmetric composite plates while Figure 7.4 shows the effect of the number of layers for thick symmetric and anti-symmetric composite plates.

Several response behaviours to the number of layer parameter of angle-ply composite plates can be observed here. Firstly the figures show that as the numbers of layer are increased, the NDTcr increased too for each angles. The increment is at the greatest for the angle of  $\theta = 45^0$ . As such, the figures also show that in all cases, the NDTcr are maximum at  $\theta = 45^0$ . Secondly, it is obvious however that the amount of increment of the NDTcr is reduced as the numbers of layers are increased. This is due to the well-known coupling effects of the composite that are reduced to zero as the numbers of layer are increased. It can also be seen that the thick composites give higher values of NDTcr as compared to the thin composites. Also by comparing cases by cases between symmetric and anti-symmetric composites, the NDTcr values are slightly different not only due to the fact that they are either symmetric or anti-symmetric, but also to the slightly different numbers of layers that they have.

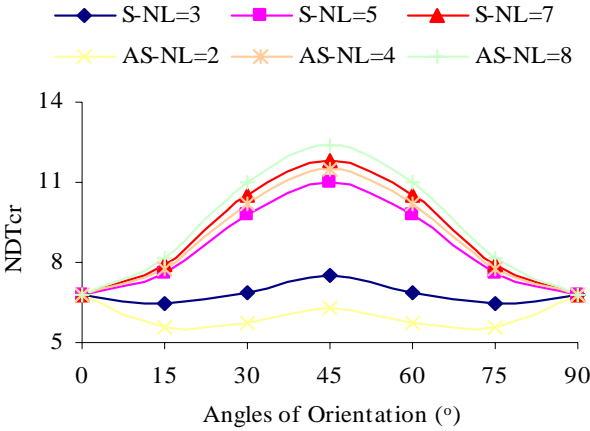


**Figure 7.3.** The effect of the number of layers (NL) on the NDTcr for *thin* symmetric (S) and anti-symmetric (AS) composite plates ( $a/t=100$ )

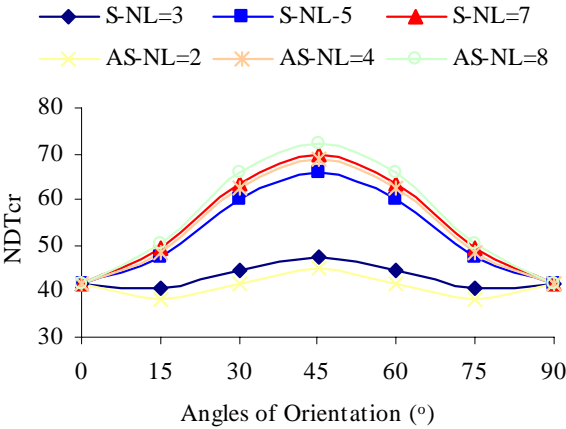


**Figure 7.4.** The effect of the number of layers (NL) on the NDTcr for *thick* symmetric (S) and anti-symmetric (AS) composite plates ( $a/t=10$ )

### 1.2.2 The effect of the level of anisotropy

The level of anisotropy is indicated by the ratio of  $E_1/E_2$ . It indicates the deviation of the anisotropic composites from the isotropic plates. Increasing the level of anisotropy will stiffen the laminate. The HH boundary condition was used in this study. The results are shown in Figure 7.5 and 7.6 for thin and thick composites respectively. As expected, both figures show that as the ratios of  $E_1/E_2$  are increased, the  $NDT_{cr}$  also increased for each angle of orientation,  $\theta$ . As in the previous studies, the maximum  $NDT_{cr}$  occurs at the angle of  $45^\circ$ .

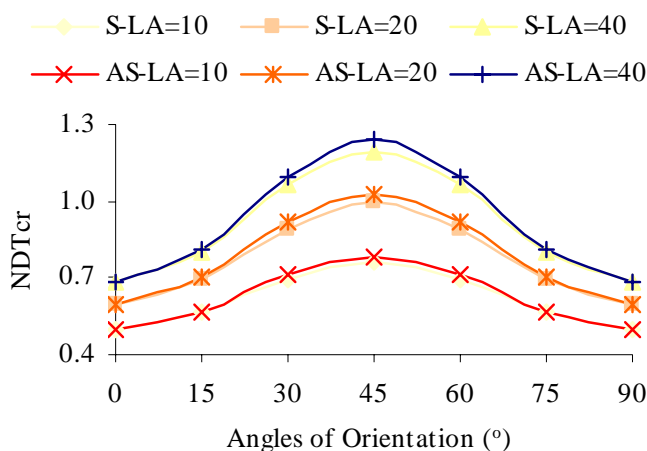


**Figure 7.5.** The effect of the level of anisotropy (LA) ie.  $E_1/E_2$  on the  $NDT_{cr}$  for *thin* symmetric (S) and anti-symmetric (AS) composite plates ( $a/t=100$ ).

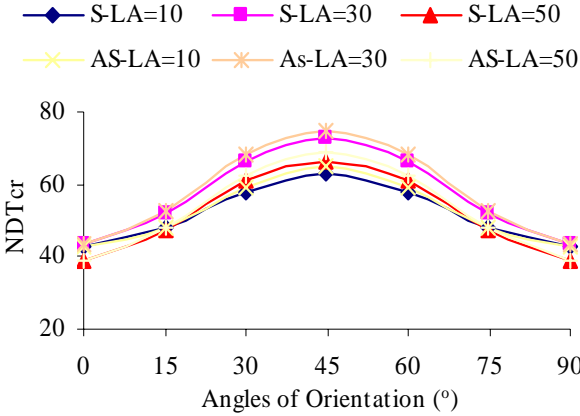


**Figure 7.6.** The effect of the level of anisotropy (LA) i.e.  $E_1/E_2$  on the NDTcr for *thick* symmetric (S) and anti-symmetric (AS) composite plates ( $a/t=10$ )

### 1.2.3 The effect of the boundary conditions

The effect of boundary conditions on the thermal buckling of plates was studied. The two types of boundary conditions, HH and CC were considered here. It can be seen in both Figure 7.6 and 7.6 which correspond to the response behaviours of thin and thick composites respectively, that the CC boundary condition gives the higher NDTcr compared to the results given by the HH boundary condition. It can also be seen in Figure 7.7 that the CC boundary condition gives the points of minimum responses at  $T = 45^{\circ}\text{C}$  while the HH boundary conditions gives the point of maximum responses at  $T = 45^{\circ}\text{C}$ . Figure 7.8 however shows the points of maximum responses for both HH and CC boundary conditions.

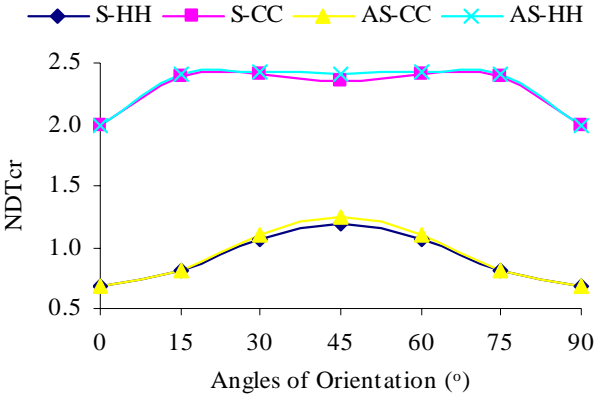


**FIGURE 7.7.** The effect of the boundary condition on the non-dimensionalised thermal critical loads for *thin* symmetric (S) and anti-symmetric (AS) composite plates ( $a/t=100$ ).

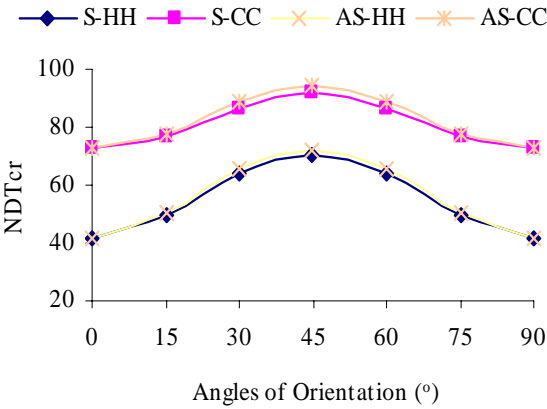


**FIGURE 7.8.** The effect of the boundary condition on the non-dimensionalised critical thermal buckling loads for *thick* symmetric (S) and anti-symmetric (AS) composite plates ( $a/t=10$ ).

#### 1.2.4 The effect of plate thickness

In this study, the side  $a$  over thickness ratios ( $a/t$ ) were varied to see the effect on the thermal buckling loads of the composite plates. The  $a/b$  ratio of 1 and the HH boundary condition are used here. Only the angle  $\theta$ s of  $30^\circ$  and  $45^\circ$  were studied. The results are shown in Figure 7.9 for both symmetric and anti-symmetric composite plates. In can be seen that as the thickness is reduced i.e, the  $a/t$  ratios are increased, the  $NDT_{cr}$  is reduced in quite a fast manner. It is also shown in the graph that the  $NDT_{cr}$  is reduced to almost zero in all cases only at the ratio  $a/t$  equal to 60.

#### 1.2.5 The effect of the aspect ratios

In this study, the ratios of side lengths,  $a/b$  were varied to see the variation of  $NDT_{cr}$  for both thin and thick symmetric and anti-symmetric angle-ply composite plates. The HH boundary condition was used here. Figure 7.10 and 7.11 shows that for both thin and thick composites, the  $NDT_{cr}$  increased as the  $a/b$  ratios increased where the effect is more significant for thick plates.

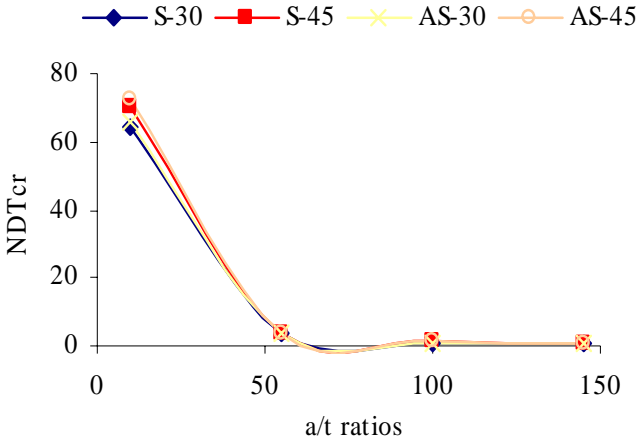


**Figure 7.9.** The effect of the side to thickness ratios on the  $NDT_{cr}$  for symmetric (S) and anti-symmetric (AS) angle-ply composite plates with  $\theta=30^\circ$  and  $45^\circ$ .



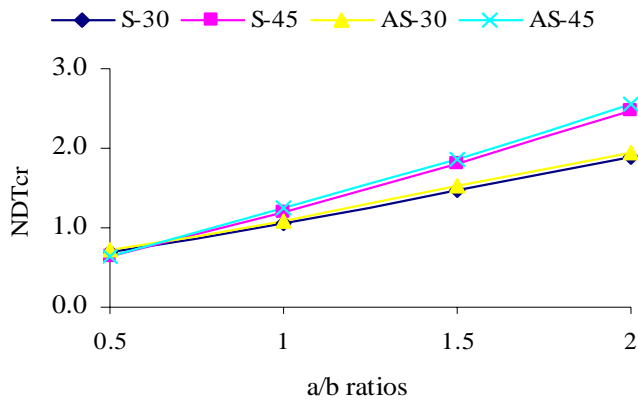


**Figure 7.10.** The effect of the aspect ratios on the NDTcr for symmetric (S) and anti-symmetric (AS) angle-ply composite plates with  $\theta = 30^\circ$  and  $45^\circ$ .

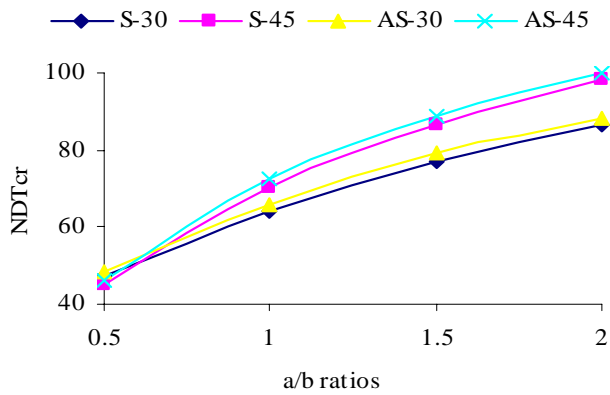


**FIGURE 7.11.** The effect of the aspect ratios on the NDTcr for symmetric (S) and anti-symmetric (AS) angle-ply composite plates with  $\theta = 30^\circ$  and  $45^\circ$ .

### 1.3 CONCLUSION

A simple finite element model and its source codes were developed to study the thermal buckling behaviour of laminated composite plates. It is found that this model and the corresponding source codes are able to describe the behaviour of thermal buckling of symmetric and anti-symmetric angle-ply composite plates when several parameters are varied. In general the NDTcr for the symmetric and anti-symmetric angle-ply composites is maximum at the angle  $\theta$  of  $45^\circ$ . As the numbers of layers are increased, the NDTcr are increased along for every  $\theta$  of the angle-ply composite plates. The similar behaviour can be seen if the  $E_1/E_2$  ratios are increased. The CC boundary condition gives higher NDTcr as compared to the values given by the HH boundary condition. The NDTcr reduces to almost zero in a quick manner when the thickness of the plate is reduced. On the other hand, the NDTcr increased as the  $a/b$  ratios are increased.

### REFERENCES

- 1) L. Librescu, W. Lin, M.P. Nemeth and J.H.Starnes, Jr. 1994. Effects Of Tangential Edge Constraints On The Post-Buckling Behaviour Of Flat And Curved Panels Subjected To Thermal And Mechanical Loads, *International Mechanical Engineering Congress and Exposition*, Chicago, Illinois.
- 2) V.S. Thankam, G. Singh, G.V. Rao, and A. K. Rath. 2003. Thermal Post-Buckling Behaviour Of Laminated Plates Using A Shear-Flexible Element Based On Coupled-Displacement Field, *Composite Structures*, 59, , 351– 359.

- 3) M.R. Prabhu and R. Dhanaraj. 1994. Thermal Buckling Of Laminated Composite Plates. *Computer and Structures*, 53(5), 1193– 1204.
- 4) C.A. Shankara, and N.G.R. Iyengar. 1993. Finite Element Model for the Thermo-Mechanical Buckling Analysis Of Composite Plates, *Composite Material Technology: American Society of Mechanical Engineers, Petroleum Division (Publication) PD*, 53, 293-301.
- 5) J.S. Chang. 1990. FEM Analysis Of Buckling And Thermal Buckling Of Anti-Symmetric Angle-Ply Laminates According To Transverse Shear And Normal Deformable High Order Displacement Theory, *Computer and Structures*, 37(6), 925– 946.
- 6) W.J. Chen, P.D. Lin, and L.W. Chen. 1991. Thermal Buckling Behaviour Of Thick Composite Laminated Plates Under Non-Uniform Temperature Distribution, *Computer and Structures*, 41(4), 637–645.
- 7) J.N. Reddy. 2002. *Mechanics of Composite Plates and Shells: Theory and Analysis*, 2<sup>nd</sup> Edition, New York: CRC Press.
- 8) B.A. Boley and J.J. Weiner. 1960. *Theory of Thermal Stresses*, New York: John Wiley.